

Comparison of local density functionals based on electron gas and finite systems

M. T. Entwistle,¹ M. Casula,² and R. W. Godby¹

¹*Department of Physics, University of York, and European Theoretical Spectroscopy Facility, Heslington, York YO10 5DD, United Kingdom*

²*Institut de Minéralogie, de Physique des Matériaux et de Cosmochimie (IMPMC), Sorbonne Université, CNRS UMR 7590, IRD UMR 206, MNHN, 4 Place Jussieu, 75252 Paris, France*



(Received 26 March 2018; published 25 June 2018)

A widely used approximation to the exchange-correlation functional in density functional theory is the local density approximation (LDA), typically derived from the properties of the homogeneous electron gas (HEG). We previously introduced a set of alternative LDAs constructed from one-dimensional systems of one, two, and three electrons that resemble the HEG within a finite region. We now construct a HEG-based LDA appropriate for spinless electrons in one dimension and find that it is remarkably similar to the finite LDAs. As expected, all LDAs are inadequate in low-density systems where correlation is strong. However, exploring the small but significant differences between the functionals, we find that the finite LDAs give better densities and energies in high-density exchange-dominated systems, arising partly from a better description of the self-interaction correction.

DOI: [10.1103/PhysRevB.97.235143](https://doi.org/10.1103/PhysRevB.97.235143)

I. INTRODUCTION

Density functional theory [1] (DFT) is the most popular method to calculate the ground-state properties of many-electron systems [2–7]. In the widely employed Kohn-Sham [8] (KS) formalism of DFT, the real system of interacting electrons is mapped onto a fictitious system of noninteracting electrons moving in an effective local potential, with both systems having the same electron density. While in principle an exact theory, in practice the accuracy of DFT calculations is constrained by our ability to approximate the exchange-correlation (xc) part of the KS functional, whose exact form is unknown. Identifying properties of the exact xc functional that are missing in commonly used approximations is vital for further developments.

A widely used approximation is the local density approximation [8] (LDA) which assumes that the true xc functional is solely dependent on the electron density at each point in the system. LDAs are traditionally derived from knowledge of the xc energy of the homogeneous electron gas [9] (HEG), a model system where the exchange energy¹ is known analytically and the correlation energy² is usually calculated using quantum Monte Carlo simulations. LDAs have been hugely successful in many cases [2,3], however, their validity breaks down in a number of important situations [10–18], particularly when there is strong correlation. They are known to miss out some critical features that are present in the exact xc potential, such as the cancellation of the spurious electron self-interaction [19–21], or the Coulomb-type $-1/r$ decay of the xc potential far from a finite system [22,23], instead following an incorrect

exponential decay [19,23]. They also fail to capture the derivative discontinuity [24–26], the discontinuous nature of the derivative of the xc energy with respect to electron number N , at integer N .

In a previous paper [27], we introduced a set of LDAs which, in contrast to the traditional HEG LDA, were constructed from systems of one, two, and three electrons which resembled the HEG within a *finite* region. Illustrating our approach in one dimension (1D), we found that the three LDAs were remarkably similar to one another. In this paper, we construct a 1D HEG LDA through suitable diffusion Monte Carlo [28] (DMC) techniques, along with a revised set of LDAs constructed from finite systems. We compare the finite and HEG LDAs with one another to demonstrate that local approximations constructed from finite systems are a viable alternative, and explore the nature of any differences between them.

In order to test the LDAs, we employ our iDEA code [29] which solves the many-electron Schrödinger equation exactly for model finite systems to determine the exact, fully correlated, many-electron wave function. Using this to obtain the *exact electron density*, we then utilize our reverse engineering algorithm to find the exact KS system. In our calculations we use *spinless* electrons to more closely approach the nature of exchange and correlation in many-electron systems,³ which interact via the appropriately softened Coulomb repulsion [30]⁴ $(|x - x'| + 1)^{-1}$.

¹Throughout this paper, we take the exchange energy to be the exchange energy of a self-consistent Hartree-Fock calculation.

²Throughout this paper, we take the correlation energy to be the difference between the exact energy of the many-electron system and the energy of a self-consistent Hartree-Fock calculation.

³Spinless electrons obey the Pauli principle but are restricted to a single spin type. Systems of two or three spinless electrons exhibit features that would need a larger number of spin-half electrons to become apparent. For example, two spinless electrons experience the exchange effect, which is not the case for two spin-half electrons in an $S = 0$ state. Furthermore, spinless KS electrons occupy a greater number of KS orbitals.

⁴We use Hartree atomic units: $m_e = \hbar = e = 4\pi\epsilon_0 = 1$.

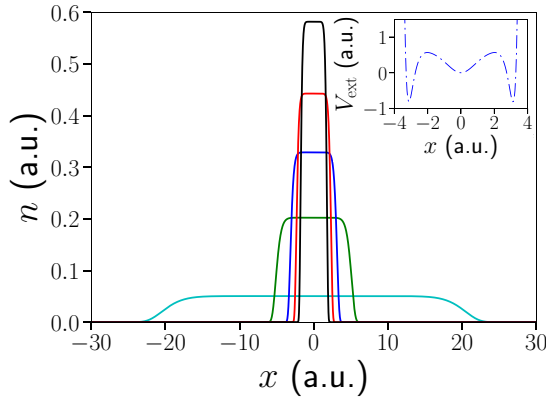


FIG. 1. The exact many-body electron density (solid lines) for a selection of the two-electron slab systems. The density is locally homogeneous across a plateau region and decays exponentially at the edges. Inset: the external potential for a typical two-electron slab system (middle density in main figure).

II. SET OF LDAS

A. LDAs from finite systems

In Ref. [27] we chose a set of finite locally homogeneous systems in order to mimic the HEG, which we referred to as “slabs” (Fig. 1). We generated sets of one-electron ($1e$), two-electron ($2e$), and three-electron ($3e$) slab systems over a typical density range (up to 0.6 a.u.) and in each case calculated the exact xc energy E_{xc} . From this we parametrized the xc energy density $\varepsilon_{xc} = E_{xc}/N$ in terms of the electron density of the plateau region of the slabs, repeating for the $1e$, $2e$, and $3e$ set.

To approximate the xc energy of an inhomogeneous system, the LDA focuses on the local electron density at each point in the system:

$$E_{xc}^{\text{LDA}}[n] = \int n(x)\varepsilon_{xc}(n) dx, \quad (1)$$

where in a conventional LDA $\varepsilon_{xc}(n)$ is the xc energy density of a HEG of density n . This approximation becomes exact in the limit of the HEG, and so it is a reasonable requirement for the finite LDAs to become exact in the limit of the slab systems. Due to the initial parametrization of $\varepsilon_{xc}(n)$ focusing on the plateau regions of the slabs (i.e., ignoring the inhomogeneous regions at the edges), we used a *refinement process* [27] in order to fulfill this requirement.

The refined form for the xc energy density in the three finite LDAs has now been increased from the four-parameter fit in Ref. [27] to a seven-parameter fit⁵ in this paper:

$$\varepsilon_{xc}(n) = (A + Bn + Cn^2 + Dn^3 + En^4 + Fn^5)n^G, \quad (2)$$

⁵We have significantly increased the precision of the calculations for the slab systems in order to do this. The numerical difference between the new seven-parameter fits and original four-parameter fits is less than 1% in ε_{xc} across the density range used in constructing the LDAs (except in the very low-density region $n < 0.06$ a.u.). This has allowed us to resolve the differences between the four LDAs in fine detail.

TABLE I. Optimal fit parameters for $\varepsilon_{xc}(n)$ in the finite LDAs. The last two rows contain the mean absolute error (MAE) and root-mean-square error (RMSE) of the fits. $\varepsilon_{xc}(n)$ is graphed in Sec. IID below.

Parameter	1e value	2e value	3e value
A	-1.2202	-1.0831	-1.1002
B	3.6838	2.7609	2.9750
C	-11.254	-7.1577	-8.1618
D	23.169	12.713	15.169
E	-26.299	-12.755	-15.776
F	12.282	5.3817	6.8494
G	7.4876×10^{-1}	7.0955×10^{-1}	7.0907×10^{-1}
MAE	1.3×10^{-4}	1.2×10^{-4}	9.9×10^{-5}
RMSE	1.9×10^{-3}	5.1×10^{-4}	3.8×10^{-4}

where the optimal parameters for each LDA are given in Table I. The xc potential V_{xc} is defined as the functional derivative of the xc energy which in the LDA reduces to a simple form (see Supplemental Material [31])

$$V_{xc}^{\text{LDA}}(n) = \varepsilon_{xc}(n(x)) + n(x) \frac{d\varepsilon_{xc}}{dn} \Big|_{n(x)}. \quad (3)$$

B. HEG exchange functional

In Ref. [27] we solved the Hartree-Fock equations to find the exact exchange energy density ε_x for a fully spin-polarized [$\zeta = 1$ where $\zeta \equiv (N^\uparrow - N^\downarrow)/N$] 1D HEG of density n consisting of an infinite number of electrons interacting via the softened Coulomb repulsion $u(x - x') = (|x - x'| + 1)^{-1}$:

$$\varepsilon_x(n) = -\frac{1}{8\pi^2 n} \int_{-\pi n}^{\pi n} dk \int_{-\pi n}^{\pi n} dk' u(k' - k), \quad (4)$$

where the Fourier transform of $u(x - x')$ is integrated over the plane defined by the Fermi wave vector $k_F = \pi n$.

Solving Eq. (4) for the range of densities we used in the finite LDAs, we parametrized $\varepsilon_x(n)$. Once again, we have increased our fit from four parameters to seven parameters, as in Eq. (2) above (see Supplemental Material [31]). The optimal parameters are given in Table II. The $\varepsilon_x(n)$ curve is shown in the inset of Fig. 2.

TABLE II. Optimal fit parameters for $\varepsilon_x(n)$ in the HEG LDA. The last two rows contain the mean absolute error (MAE) and root-mean-square error (RMSE) of the fit.

Parameter	Value
A	-1.1511
B	3.3440
C	-9.7079
D	19.088
E	-20.896
F	9.4861
G	7.3586×10^{-1}
MAE	6.5×10^{-5}
RMSE	7.2×10^{-4}

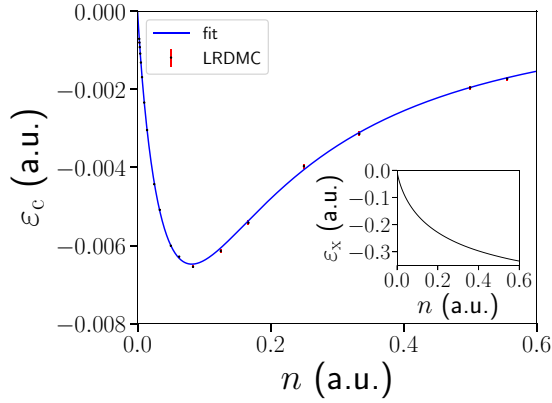


FIG. 2. The ε_c (with associated error bars) for a set of HEGs over the density range used in the finite LDAs. The fit applied (solid blue) becomes exact in the known high- and low-density limits. Inset: the ε_x curve in the HEG LDA.

C. HEG correlation functional

We use the lattice regularized diffusion Monte Carlo (LRDMC) algorithm [28] to compute the ground-state energy of the fully spin-polarized HEG over a wide range of densities, much higher than the 0.6 a.u. limit used in the finite LDAs. This is in order to ensure the resultant parametrization of the correlation energy density ε_c reduces to the known high- and low-density limits. We determine ε_c by subtracting the kinetic energy and ε_x contributions from the total energy.

To parametrize the correlation energy density we use a fit of the form (see Supplemental Material [31])

$$\varepsilon_c(r_s) = -\frac{A_{\text{RPA}}r_s + Er_s^2}{1 + Br_s + Cr_s^2 + Dr_s^3} \frac{\ln(1 + \alpha r_s + \beta r_s^2)}{\alpha}, \quad (5)$$

where r_s is the Wigner-Seitz radius and is related to the density (in 1D) by $2r_s = 1/n$. The optimal parameters (with estimated errors) are given in Table III. The fit applied to the data is shown in Fig. 2.

The high-density limit (infinitely weak correlation) of the parametrization is

$$\varepsilon_c(r_s \rightarrow 0) = -A_{\text{RPA}}r_s^2, \quad (6)$$

and its low-density limit (infinitely strong correlation) is

$$\varepsilon_c(r_s \rightarrow \infty) = -\frac{2E}{\alpha D} \frac{\ln(r_s)}{r_s}. \quad (7)$$

Therefore, the parametric form in Eq. (5) correctly reproduces the expected behavior of the correlation energy density in the high-density limit [$\varepsilon_c \propto r_s^2$] and low-density limit [$\varepsilon_c \propto \ln(r_s)/r_s$].

D. Comparison of 1e, 2e, 3e, and HEG LDAs

Summing together the HEG exchange and correlation parametric fits, we can now compare the HEG LDA that we have developed against the three finite LDAs. The striking similarity between the four ε_{xc} curves can be seen in Fig. 3(a). While very similar in the low-density range, there are some differences between them. These are highlighted in Fig. 3(b) which, using the 1e LDA as a reference, plots its difference with

TABLE III. Optimal fit parameters with estimated errors in parentheses for $\varepsilon_c(r_s)$ in the HEG LDA. The last two rows contain the mean absolute error (MAE) and root-mean-square error (RMSE) of the fit. Note: A_{RPA} has been determined from the high-density limit for ε_c (in which the random phase approximation (RPA) is exact [32,33]), which is exactly fulfilled by our fit, and hence has no associated error.

Parameter	Value
A_{RPA}	9.415195×10^{-4}
B	$2.601(5) \times 10^{-1}$
C	$6.404(7) \times 10^{-2}$
D	$2.48(3) \times 10^{-4}$
E	$2.61(3) \times 10^{-6}$
α	1.254(2)
β	28.8(1)
MAE	2.4×10^{-5}
RMSE	1.3×10^{-4}

the remaining LDAs. There is a competing balance between exchange and correlation. At low densities, these differences can be mainly attributed to ε_c , which is entirely absent in the 1e LDA, and increases in magnitude as we progress to 2e to 3e to HEG (Fig. 4). As we move to higher densities in which the magnitude of ε_c decreases, and the magnitude of ε_x increases, the order of the four ε_{xc} curves reverses. They increasingly separate as we move to higher densities with the 1e LDA, which consists entirely of self-interaction correction, giving the

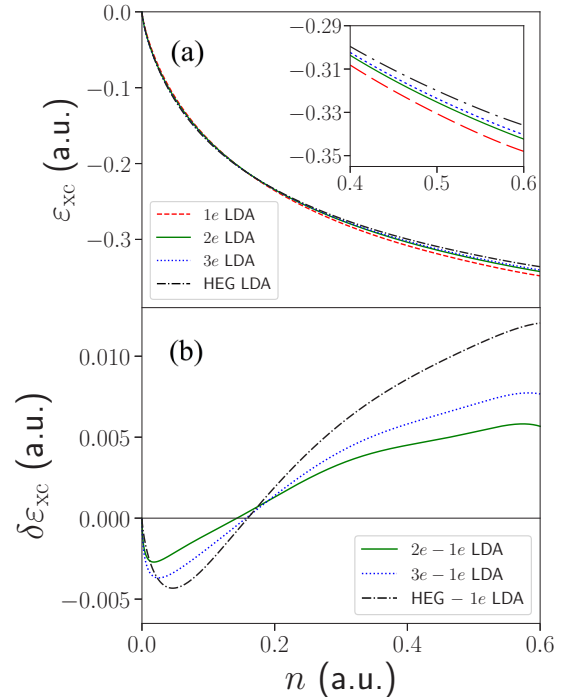


FIG. 3. (a) The ε_{xc} curves in the 1e (dashed red line), 2e (solid green line), 3e (dotted blue line), and HEG (dotted-dashed black line) LDAs. Inset: closeup of the four curves at higher densities. The similarity between them is striking, with a clear progression from 1e to 2e to 3e to HEG. (b) The 1e LDA is used as a reference here. Plotted is its difference ($\delta\varepsilon_{xc} = \varepsilon_{xc} - \varepsilon_{xc}^{1e}$) with the 2e (solid green line), 3e (dotted blue line), and HEG (dotted-dashed black line) LDAs.

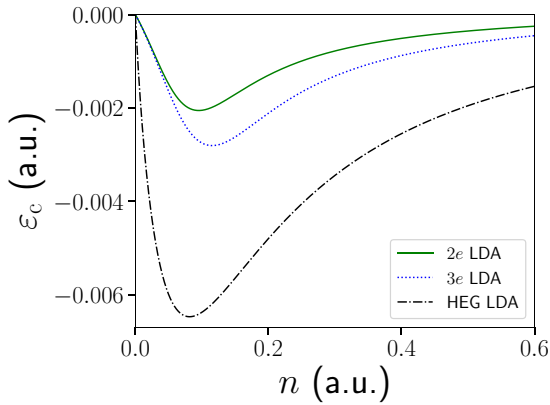


FIG. 4. We calculate the exact ε_c for the $2e$ (solid green line) and $3e$ (dotted blue line) slab systems through Hartree-Fock calculations. We plot these against the ε_c curve in the HEG LDA (dotted-dashed black line). The ε_c in the HEG LDA is much larger (~ 2 – 3 that of the $3e$ LDA and ~ 3 – 4 that of the $2e$ LDA). While not a perfect comparison due to the refinement process used in the construction of the finite LDAs, it gives a useful indication of the size of ε_c in their ε_{xc} curves.

largest magnitude for ε_{xc} . By plotting the difference between the $1e$ LDA (where correlation is absent) and the exchange part of the HEG LDA (i.e., removing the correlation term), it can be seen that the $1e$ LDA yields a larger exchange energy density than the HEG LDA at all densities (Fig. 5).

The refinement process used in the construction of the finite LDAs focused on giving the correct E_{xc} in the limit of the slab systems, but did not ensure that the correct V_{xc} , and by extension electron density, were reproduced (a property of HEG LDAs). We find that the finite LDAs are completely inadequate at reproducing the densities of the slab systems. We compare the *exact* V_{xc} against n and find that there is a high nonlocal dependence on n , implying that *no* local density functional can accurately reproduce V_{xc} and hence n for the slab systems. In light of this, the success of the finite LDAs reported below is all the more surprising.

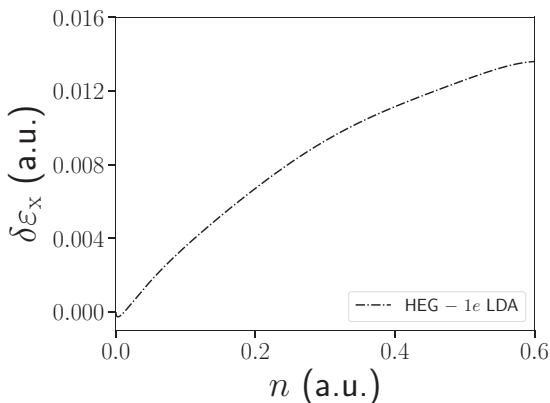


FIG. 5. The ε_x curve in the $1e$ LDA ($\varepsilon_x = \varepsilon_{xc}$) is used as a reference here. Plotted is its difference ($\delta\varepsilon_x = \varepsilon_x - \varepsilon_x^{1e}$) with the ε_x curve in the HEG LDA ($\varepsilon_x = \varepsilon_{xc} - \varepsilon_c$). It can be seen that the $1e$ LDA yields a larger exchange energy density than the HEG LDA at all densities. Note: This is not true in the very low-density region ($n < 0.012$), which we attribute to errors in the fits.

III. TESTING THE LDAs

In the previous section we observed the close similarity between the four LDAs. In this section we apply them to a range of model systems (see Supplemental Material [31]) in order to identify the differences between them.

A. Weakly correlated systems

System 1 (2e harmonic well). We first consider a pair of interacting electrons in a strongly confining harmonic potential well ($\omega = \frac{2}{3}$ a.u.) where correlation is very weak.⁶ We calculate the exact many-body electron density using iDEA, and compare it against the densities obtained from applying the LDAs self-consistently. There is a progression from the $1e$ – $2e$ – $3e$ –HEG LDA and so we choose to plot the $1e$ and HEG LDA densities (i.e., the $2e$ and $3e$ LDA densities lie between these) against the exact [Fig. 6(a)]. Both LDAs match the exact density well, and so we plot their absolute errors ($\delta n = n^{\text{LDA}} - n^{\text{exact}}$) to more clearly identify their differences [Fig. 6(b)]. The $1e$ LDA has a slightly smaller net absolute error ($\int |\delta n| dx$). While the HEG LDA gives a slightly better electron density in the central region (dip in the density), the $1e$ LDA better matches the decay of the density towards the edges of the system, and perhaps more interestingly, the two peaks in the density where the self-interaction correction is largest.

Due to the importance of energies in DFT calculations, we also compare the exact E_{xc} and total energy E_{total} , with those obtained from applying the LDAs self-consistently (Table IV). While all the LDAs give good approximations to both quantities, there are some significant differences due to this system being dominated by regions of high density, and the ε_{xc} curves separating in this limit (see Fig. 3). As with the approximations to the electron density, there is a progression from the $1e$ – $2e$ – $3e$ –HEG LDA, with the $1e$ LDA reducing the absolute errors ($\frac{\delta E_{xc}}{E_{xc}}, \frac{\delta E}{E}$) in the HEG LDA by a factor of 5–6.

System 2 (3e harmonic well). Next, we consider a harmonic potential well with three electrons, but slightly less confining ($\omega = \frac{1}{2}$), in order to avoid an unphysically high electron density ($n > 0.6$ a.u.). As in the $2e$ harmonic well system, we find a progression from the $1e$ – $2e$ – $3e$ –HEG LDA, with all LDAs giving good electron densities [see Fig. 7(a) for the $1e$ and HEG LDA densities plotted against the exact]. Again, the $1e$ LDA has the smallest net absolute error, and outperforms the rest of the LDAs in the regions where the density peaks [Fig. 7(b)].

We also compare the exact E_{xc} and E_{total} against the LDAs (Table IV). All LDAs give good energies, with some noticeable differences between them due to this system being dominated by regions of high density, like in the $2e$ harmonic well system. However, the *magnitude* of E_{xc} in the $1e$ LDA is greater than the exact (i.e., it overestimates the amount of exchange + correlation), and subsequently it gives a total energy lower than the exact. While the absolute error in E_{xc} for each LDA is similar to that in E_{total} , this overestimation of exchange +

⁶We calculate the absolute error between the exact electron density and the density obtained from a self-consistent Hartree-Fock calculation ($\delta n = n^{\text{HF}} - n^{\text{exact}}$), and find the net absolute error to be $\int |\delta n| dx \approx 1.4 \times 10^{-3}$. The correlation energy is 0.13% of the exchange-correlation energy -0.62 a.u.

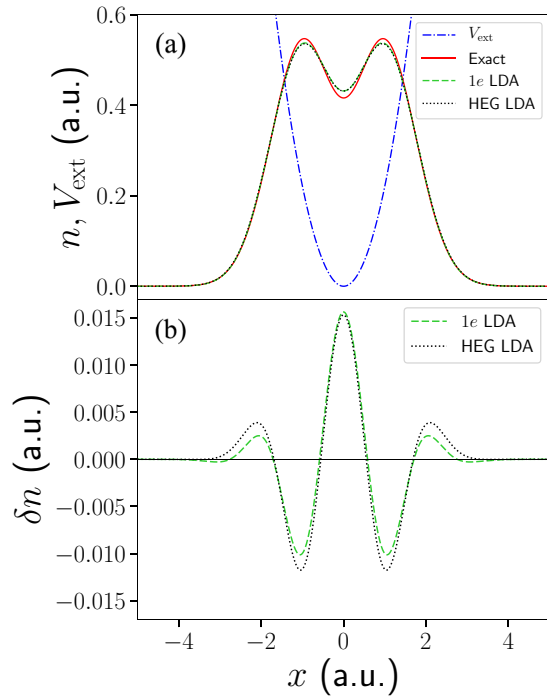


FIG. 6. System 1 (two electrons in a harmonic potential well). (a) The external potential (dotted-dashed blue line), together with the exact electron density (solid red line), and the densities obtained from applying the $1e$ (dashed green line) and HEG (dotted black line) LDAs. Both LDAs are in very good agreement with the exact result. (b) The absolute error in the density ($\delta n = n^{\text{LDA}} - n^{\text{exact}}$) in the $1e$ (dashed green line) and HEG (dotted black line) LDAs, allowing their differences to be more clearly identified.

correlation in the $1e$ LDA results in the $2e$ LDA giving the best total energy.

B. A system dominated by the self-interaction correction

The self-interaction correction (SIC) is *absent* in xc functionals constructed from the HEG. However, the xc energy of the $1e$ slab systems (which were used to construct the $1e$ LDA) consists entirely of SIC. In the first two model systems, we found that the $1e$ LDA (and indeed the other finite LDAs) better describes the electron density in regions where the SIC is strongest, than the HEG LDA. We now investigate this further.

System 3 (2e double well). We choose a system with two electrons confined to a double-well potential. The wells are separated, such that the electrons are *highly localized* and can be considered as two separate subsystems [Fig. 8(a)]. This

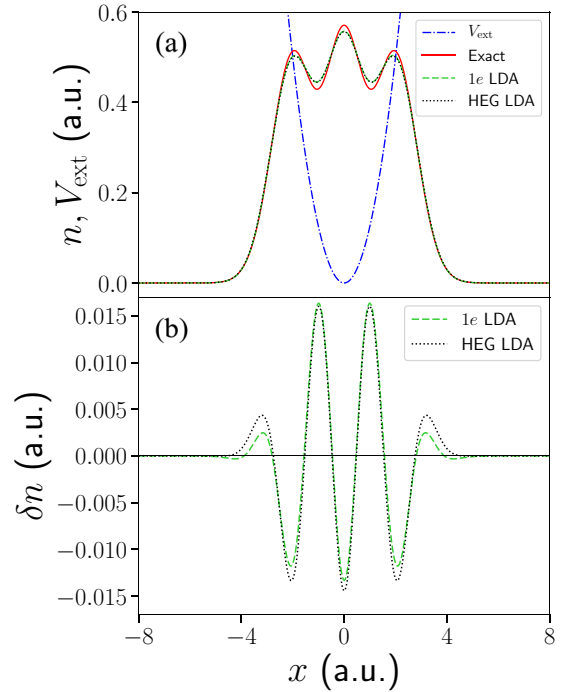


FIG. 7. System 2 (three electrons in a harmonic potential well). (a) The external potential (dotted-dashed blue line), together with the exact electron density (solid red line), and the densities obtained from applying the $1e$ (dashed green line) and HEG (dotted black line) LDAs. Much like the $2e$ harmonic well system, both LDAs match the exact density well. (b) The absolute error in the density in the $1e$ (dashed green line) and HEG (dotted black line) LDAs. Again, the $1e$ LDA outperforms the HEG LDA in the density peaks, which is dominated by the self-interaction correction.

results in the Hartree potential being small outside of the wells, and being dominated by the electron self-interaction within the wells. Consequently, a large proportion of the xc potential is self-interaction correction. Applying the LDAs, we find the usual progression $1e-2e-3e$ -HEG. Focusing on the peaks in the electron density, the $1e$ LDA substantially reduces the error present in the HEG LDA [Fig. 8(b)]. To understand this, we analyze the xc potential [Fig. 8(c)]. The $1e$ LDA better reproduces the large dips in V_{xc} , corresponding to the peaks in the electron density. Hence, the SIC is more effectively captured.

While the LDA errors in E_{xc} are larger than in the first two systems, they are still small (4.8%–6.8%) (Table IV). The absolute errors in E_{total} are similar.

TABLE IV. Total energies and xc energies for the set of weakly correlated systems (1–3), from exact calculations and from applying the four LDAs self-consistently ($\delta E^{\text{LDA}} = E^{\text{LDA}} - E^{\text{exact}}$). Estimated errors are ± 1 in the last decimal place, unless otherwise stated in parentheses.

System	E_{total} (a.u.)					E_{xc} (a.u.)				
	Exact	$\delta E_{\text{total}}^{1e}$	$\delta E_{\text{total}}^{2e}$	$\delta E_{\text{total}}^{3e}$	$\delta E_{\text{total}}^{\text{HEG}}$	Exact	δE_{xc}^{1e}	δE_{xc}^{2e}	δE_{xc}^{3e}	$\delta E_{xc}^{\text{HEG}}$
$2e$ harmonic well	1.6932	0.0037	0.0126	0.0153	0.0211	−0.6192	0.0045	0.0137	0.0165	0.0225
$3e$ harmonic well	3.1875	−0.0073	0.0065	0.0108	0.0199	−0.9305(5)	−0.0058(5)	0.0085(5)	0.0129(5)	0.0223(5)
$2e$ double well	−1.0301	0.0237	0.0286	0.0296	0.0323	−0.5349	0.0256	0.0317	0.0331	0.0363

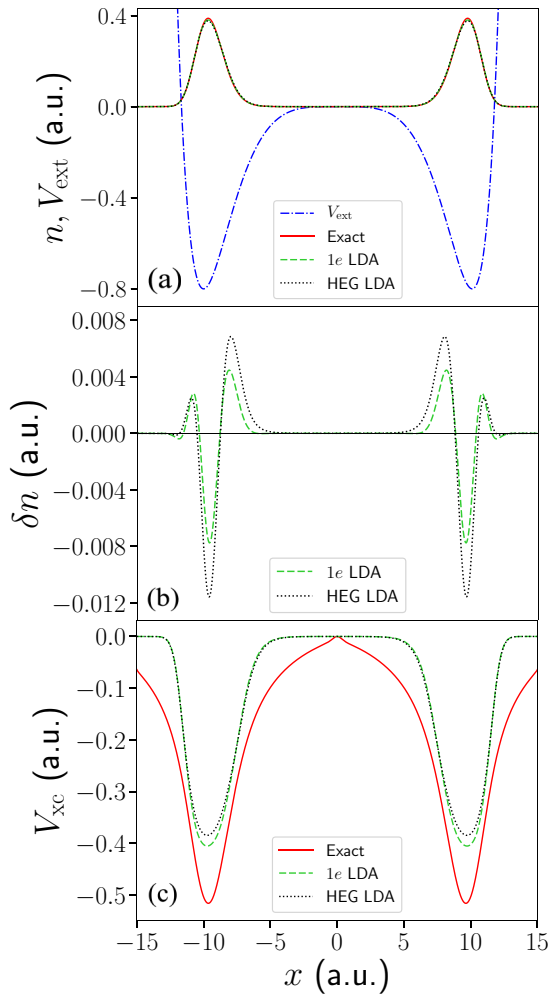


FIG. 8. System 3 (two electrons in a double-well potential). (a) The external potential (dotted-dashed blue line), together with the exact electron density (solid red line), and the densities obtained from applying the $1e$ (dashed green line) and HEG (dotted black) LDAs. The wells are separated, such that the electrons are highly localized. (b) The absolute error in the density in the $1e$ (dashed green line) and HEG (dotted black line) LDAs. The $1e$ LDA is far superior in the regions where the density peaks, and hence where the Hartree potential is large and dominated by the electron self-interaction. (c) The exact xc potential (solid red line), and the xc potentials given by the $1e$ (dashed green line) and HEG (dotted line) LDAs. The dips in V_{xc} are more closely matched by the $1e$ LDA due to it better capturing the self-interaction correction, present in the exact V_{xc} .

C. Systems where correlation is stronger

System 4 (2e atom). We now consider a system where the relative size of electron correlation increases significantly:⁷ two electrons confined to a *softened* atomiclike potential $V_{\text{ext}} = -(|ax| + 1)^{-1}$, where $a = \frac{1}{20}$. Although we find the same

⁷We calculate the absolute error between the exact electron density and the density obtained from a self-consistent Hartree-Fock calculation ($\delta n = n^{\text{HF}} - n^{\text{exact}}$), and find the net absolute error to be $\int |\delta n| dx \approx 7.4 \times 10^{-2}$. The correlation energy is 1.1% of the exchange-correlation energy -0.37 a.u.

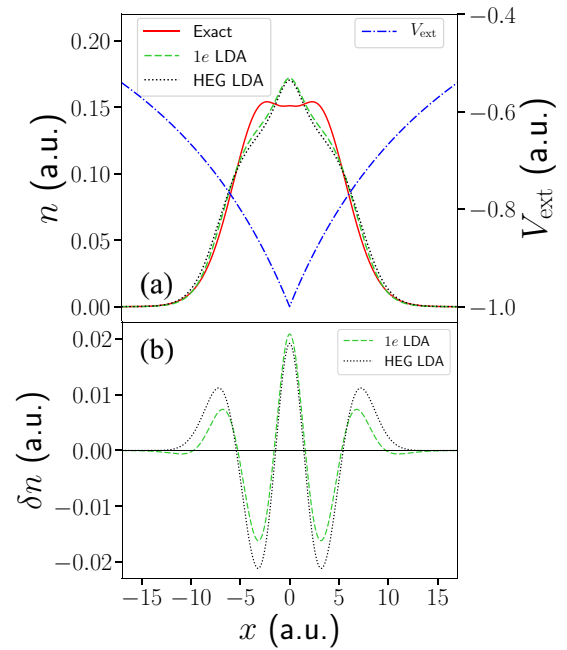


FIG. 9. System 4 (two electrons in a softened atomiclike potential). (a) The external potential (dotted-dashed blue line), together with the exact electron density (solid red line), and the densities obtained from applying the $1e$ (dashed green line) and HEG (dotted black line) LDAs. Unlike in the weakly correlated systems, the LDAs give poor electron densities. (b) The absolute error in the density in the $1e$ (dashed green line) and HEG (dotted black line) LDAs. While the net absolute errors are much larger than in the weakly correlated systems, the $1e$ LDA still performs the best.

progression ($1e-2e-3e-HEG$) as seen in the first three model systems, in which correlation was weak, all LDAs give inadequate electron densities. This can be seen by plotting the $1e$ and HEG LDA densities against the exact [Fig. 9(a)]. The LDAs give densities that are not even qualitatively correct, e.g., predicting a single peak in the center of the system, which is absent in the exact density. The net absolute errors are much larger than in the weakly correlated systems, however, the $1e$ LDA once again gives the smallest [Fig. 9(b)].

We find that although the LDA densities are poor, the xc energies are surprisingly good (Table V). This can be attributed *somewhat* (see Sec. III D for investigation of further causes) to errors in the density being partially canceled by errors inherent in the approximate xc energy functional [34]. We infer this by noting the progression (HEG- $3e-2e-1e$) when we apply the LDAs to the *exact* density, in contrast to the self-consistent solutions in Table V. As in the weakly correlated systems, the absolute errors in E_{total} are smaller than in E_{xc} , due to a partial cancellation of errors from the Hartree energy component. It is much more apparent in this system due to the LDAs incorrectly predicting a central peak in the electron density [Fig. 9(a)].

System 5 (3e atom). Finally, we consider three electrons in an external potential of the same form as the $2e$ atom, but less confining, with $a = \frac{1}{50}$. Along with the usual progression ($1e-2e-3e-HEG$), we find a similar result to the $2e$ atom, with the LDAs giving poor electron densities [Fig. 10(a)]. Although the densities are qualitatively correct, unlike in the

TABLE V. Total energies and xc energies for the set of strongly correlated systems (4 and 5), from exact calculations and from applying the four LDAs self-consistently ($\delta E^{\text{LDA}} = E^{\text{LDA}} - E^{\text{exact}}$). Estimated errors are ± 1 in the last decimal place, unless otherwise stated in parentheses.

System	E_{total} (a.u.)					E_{xc} (a.u.)				
	Exact	$\delta E_{\text{total}}^{1e}$	$\delta E_{\text{total}}^{2e}$	$\delta E_{\text{total}}^{3e}$	$\delta E_{\text{total}}^{\text{HEG}}$	Exact	$\delta E_{\text{xc}}^{1e}$	$\delta E_{\text{xc}}^{2e}$	$\delta E_{\text{xc}}^{3e}$	$\delta E_{\text{xc}}^{\text{HEG}}$
2e atom	-1.5099	0.0053	0.0044	0.0032	0.0022	-0.3728	0.0084	0.0101	0.0099	0.0111
3e atom	-2.3282(5)	0.0121(5)	0.0085(5)	0.0057(5)	0.0029(5)	-0.493(4)	0.029(4)	0.029(4)	0.027(4)	0.028(4)

2e atom, the LDAs significantly underestimate the peaks in the electron density. Subsequently, the absolute errors are very large [Fig. 10(b)]. The 1e LDA, along with giving the lowest net absolute error, most accurately reproduces the peaks in the density, where the SIC is largest.

While the absolute errors in E_{xc} are larger than in the 2e atom, they are still small (Table V). Again, this partially arises from applying approximate xc energy functionals to incorrect densities. As in the 2e atom, the absolute errors in E_{total} are much lower than those in E_{xc} , due to a partial cancellation of errors from the Hartree energy component.

D. Cancellation of errors between exchange and correlation

HEG-based LDAs have been known to typically underestimate the *magnitude* of the exchange energy E_{x} , while overestimating the magnitude of the correlation energy E_{c} . Consequently, while the total E_{xc} is underestimated in magnitude, the approximation proves to be better than was originally expected due to a partial cancellation of errors.

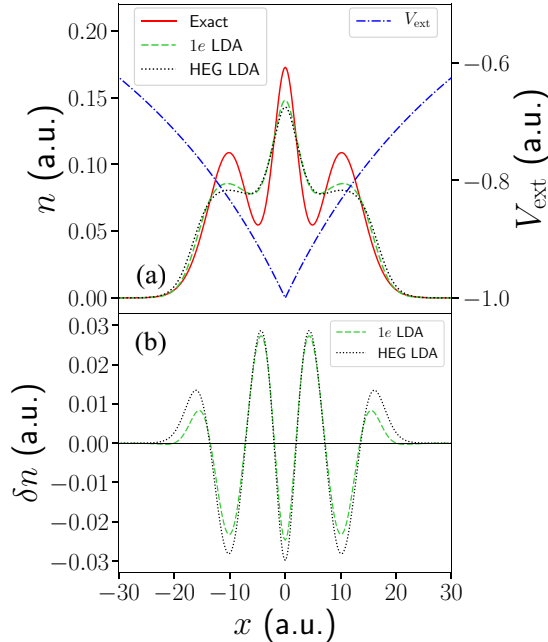


FIG. 10. System 5 (three electrons in a softened atomiclike potential). (a) The external potential (dotted-dashed blue line), together with the exact electron density (solid red line), and the densities obtained from applying the 1e (dashed green line) and HEG (dotted black line) LDAs. Like in the 2e atom, the LDAs give poor electron densities. The 1e LDA more accurately reproduces the peaks in the density, where the SIC is largest. (b) The absolute error in the density in the 1e (dashed green line) and HEG (dotted black line) LDAs. Again, the net absolute errors are large, with the 1e LDA giving the smallest.

We investigate how well our HEG LDA approximates E_{x} and E_{c} in the model systems, and how this contributes to accurate values for E_{xc} . To do this we perform Hartree-Fock calculations for each of the model systems, and together with the exact solutions obtained through iDEA, are able to divide the exact E_{xc} into its exchange and correlation components. We then apply the HEG LDA, which is split into separate E_{x} and E_{c} functionals, for comparison (Table VI). In all systems, the HEG LDA underestimates the magnitude of E_{x} , while it overestimates the magnitude of E_{c} . However, due to the exchange energy being the dominant component of E_{xc} , even in strongly correlated systems, this only leads to a partial cancellation of errors.

The 1e LDA yields a larger magnitude for ε_{x} than the HEG LDA across the entire density range studied (up to 0.6 a.u.) (Fig. 5), which arises from a better description of the SIC (Sec. III B). In the 1e LDA correlation is absent. Consequently, the 1e xc energies that follow from Tables IV and V can be considered as approximations to E_{x} . We note that the 1e LDA substantially reduces the error in E_{x} that arises in the HEG LDA.⁸ We infer that this error reduction will also extend to the 2e and 3e LDAs.

⁸This is also true in the 2e double-well system where correlation is negligible, and the exchange energy is dominated by the SIC.

TABLE VI. Exchange energies and correlation energies for all systems (1–5), from exact calculations and from applying the HEG LDA self-consistently ($\delta E^{\text{LDA}} = E^{\text{LDA}} - E^{\text{exact}}$). Estimated errors are ± 1 in the last decimal place, unless otherwise stated in parentheses.

System	E_{x} (a.u.)	
	Exact	$\delta E_{\text{x}}^{\text{HEG}}$
2e harmonic well	-0.6184	0.0268
3e harmonic well	-0.9286(5)	0.0276(5)
2e double well	-0.5349	0.0441
2e atom	-0.3686	0.0185
3e atom	-0.488(3)	0.041(3)
System	E_{c} (a.u.)	
	Exact	$\delta E_{\text{c}}^{\text{HEG}}$
2e harmonic well	-0.0008	-0.0043
3e harmonic well	-0.0019	-0.0053
2e double well	-0.0000	-0.0077
2e atom	-0.0042	-0.0074
3e atom	-0.0043(5)	-0.0142(5)

IV. CONCLUSIONS

We have constructed an LDA based on the homogeneous electron gas (HEG) through suitable quantum Monte Carlo techniques and find that it is remarkably similar in many regards to a set of three LDAs constructed from finite systems. Applying them to test systems to explore the differences between them, we find that the finite LDAs give better densities and energies in highly confined systems in which correlation is weak. Most interestingly, the LDA constructed from systems of just one electron most accurately describes the self-interaction correction. All LDAs give poor densities in systems where correlation is stronger, but give reasonably good energies, with the HEG LDA giving the best total energies. Across all test systems, the HEG LDA underestimates the magnitude of the exchange energy and overestimates the magnitude of the correlation energy, leading to a partial cancellation of errors.

As a consequence of the finite LDAs giving a better description of the self-interaction correction, we infer that they would reduce the error in the exchange energy. Furthermore, we expect that finite LDA functionals will also provide a better treatment of the SIC for spinful electrons. Their derivation and usage could lead to an improved description of the electronic structure in a variety of situations, such as at the onset of Wigner oscillations.

Data created during this research is available by request from the York Research Database [35].

ACKNOWLEDGMENTS

M.C. acknowledges the GENCI allocation for computer resources under Project No. 0906493. We thank L. Talirz for recent developments in the iDEA code, and M. Hodgson and J. Wetherell for helpful discussions.

-
- [1] P. Hohenberg and W. Kohn, *Phys. Rev.* **136**, B864 (1964).
 [2] R. Dreizler and E. Gross, *Density Functional Theory: An Approach to the Quantum Many-Body Problem* (Springer, Berlin, 2012).
 [3] R. Parr and W. Yang, *Density-Functional Theory of Atoms and Molecules*, International Series of Monographs on Chemistry (Oxford University Press, New York, 1994).
 [4] C. Fiolhais, F. Nogueira, and M. Marques, *A Primer in Density Functional Theory*, Lecture Notes in Physics (Springer, Berlin, 2003).
 [5] K. Burke, *J. Chem. Phys.* **136**, 150901 (2012).
 [6] R. M. Martin, *Electronic Structure: Basic Theory and Practical Methods* (Cambridge University Press, Cambridge, 2004).
 [7] E. Engel and R. Dreizler, *Density Functional Theory: An Advanced Course*, Theoretical and Mathematical Physics (Springer, Berlin, 2011).
 [8] W. Kohn and L. J. Sham, *Phys. Rev.* **140**, A1133 (1965).
 [9] D. M. Ceperley and B. J. Alder, *Phys. Rev. Lett.* **45**, 566 (1980).
 [10] G. Onida, L. Reining, and A. Rubio, *Rev. Mod. Phys.* **74**, 601 (2002).
 [11] M. Lein, E. K. U. Gross, and J. P. Perdew, *Phys. Rev. B* **61**, 13431 (2000).
 [12] O. Gritsenko, S. Van Gisbergen, A. Görling, E. Baerends, *et al.*, *J. Chem. Phys.* **113**, 8478 (2000).
 [13] N. T. Maitra, K. Burke, and C. Woodward, *Phys. Rev. Lett.* **89**, 023002 (2002).
 [14] K. Burke, J. Werschnik, and E. Gross, *J. Chem. Phys.* **123**, 062206 (2005).
 [15] D. Varsano, A. Marini, and A. Rubio, *Phys. Rev. Lett.* **101**, 133002 (2008).
 [16] R. O. Jones and O. Gunnarsson, *Rev. Mod. Phys.* **61**, 689 (1989).
 [17] W. E. Pickett, *Comput. Phys. Rep.* **9**, 115 (1989).
 [18] X. Gonze, P. Ghosez, and R. W. Godby, *Phys. Rev. Lett.* **78**, 294 (1997).
 [19] J. P. Perdew and A. Zunger, *Phys. Rev. B* **23**, 5048 (1981).
 [20] D. J. Tozer and N. C. Handy, *J. Chem. Phys.* **109**, 10180 (1998).
 [21] A. Dreuw, J. L. Weisman, and M. Head-Gordon, *J. Chem. Phys.* **119**, 2943 (2003).
 [22] M. Levy, J. P. Perdew, and V. Sahni, *Phys. Rev. A* **30**, 2745 (1984).
 [23] C.-O. Almbladh and U. von Barth, *Phys. Rev. B* **31**, 3231 (1985).
 [24] P. Mori-Sanchez and A. J. Cohen, *Phys. Chem. Chem. Phys.* **16**, 14378 (2014).
 [25] M. A. Mosquera and A. Wasserman, *Phys. Rev. A* **89**, 052506 (2014).
 [26] M. A. Mosquera and A. Wasserman, *Mol. Phys.* **112**, 2997 (2014).
 [27] M. T. Entwistle, M. J. P. Hodgson, J. Wetherell, B. Longstaff, J. D. Ramsden, and R. W. Godby, *Phys. Rev. B* **94**, 205134 (2016).
 [28] M. Casula, C. Filippi, and S. Sorella, *Phys. Rev. Lett.* **95**, 100201 (2005).
 [29] M. J. P. Hodgson, J. D. Ramsden, J. B. J. Chapman, P. Lillystone, and R. W. Godby, *Phys. Rev. B* **88**, 241102 (2013).
 [30] A. Gordon, R. Santra, and F. X. Kärtner, *Phys. Rev. A* **72**, 063411 (2005).
 [31] See Supplemental Material at <http://link.aps.org/supplemental/10.1103/PhysRevB.97.235143> for the parametric form of the xc potential in the finite LDAs, for the parametric form of the exchange potential in the HEG LDA, for the parameters of the model systems, and details on our calculations to obtain converged results.
 [32] M. Casula, S. Sorella, and G. Senatore, *Phys. Rev. B* **74**, 245427 (2006).
 [33] L. Shulenburger, M. Casula, G. Senatore, and R. M. Martin, *J. Phys. A: Math. Theor.* **42**, 214021 (2009).
 [34] M.-C. Kim, E. Sim, and K. Burke, *Phys. Rev. Lett.* **111**, 073003 (2013).
 [35] M. T. Entwistle, M. Casula, and R. W. Godby, (2018), doi: 10.15124/65cd1dd8-c240-45a5-9a47-0ac6ff870f51.